

Laser-assisted two-color two-photon double ionization of helium atoms

Zhizhen Zhu

Wuhan Institute of Technology

Kai Liu (✉ 12005010008@stu.wit.edu.cn)

Wuhan Institute of Technology

Xiaofan Zhang

Wuhan Institute of Technology

Ye Li

Wuhan Institute of Technology

Feng Wang

Wuhan Institute of Technology

Meiyan Qin

Wuhan Institute of Technology

Zhe Wang

Wuhan Institute of Technology

Qing Liao

Wuhan Institute of Technology

Research Article

Keywords: Strong field laser physics, Photoionization

Posted Date: April 27th, 2021

DOI: <https://doi.org/10.21203/rs.3.rs-302329/v1>

License:   This work is licensed under a Creative Commons Attribution 4.0 International License.

[Read Full License](#)

Laser-assisted two-color two-photon double ionization of helium atoms

Zhizhen Zhu¹ · Kai Liu¹ · Xiaofan Zhang¹ · Ye Li¹ · Feng Wang¹ · Meiyang Qin¹ · Zhe Wang¹ · Qing Liao¹

Received: date / Accepted: date

Abstract Correlated momentum and kinetic energy distributions of two photoelectrons in laser-assisted two-color two-photon double ionization of helium are investigated by numerically solving a one-plus-one dimensional time-dependent Schrödinger equation (TDSE). We find that the weak assisting laser field can act as an energy transferring field, resulting in burst of double ionization. More importantly, the participation of the laser photon into the double ionization reshapes the correlation patterns in the momentum and kinetic energy distributions. The laser photon can be absorbed by any one of the two electrons, providing two channels that induces destructive interference in the correlated momentum and kinetic energy distributions, which is never found in previous work.

Keywords Strong field laser physics · Photoionization

1 Introduction

Electron correlation plays a very important role in nonsequential double ionization of atoms and thus has received extensive investigations in the past three decades [1,2,3,4,5,6]. As the simplest multi-electron system, helium atoms have showed great advantages to explore electron correlation dynamics. In spite of that, the behind physical processes of double ionization of helium atoms are still complicated, since they depends strongly on the parameters of the driven pulses. While single-photon double ionization of helium atoms have been well studied both in experiment [3] and in theory[7,8,9,10,11], the investigations of two-photon and few-photon double ionization are challenging in experiment [12] and some details are still not understood fully in theory.

Kai Liu (✉)

E-mail: 12005010008@stu.wit.edu.cn

¹ Hubei Key Laboratory of Optical Information and Pattern Recognition, Wuhan Institute of Technology, Wuhan 430205, China

In two-color two-photon double ionization, the double ionization process can be divided into two steps, if the double ionization is triggered by absorption of one XUV photon and the subsequent correlation dynamics of the two photoelectrons is perturbed by the weak laser field through additional one-laser-photon absorption or emission. By isolating the photoexcitation process from the perturbation process, we can better understand the correlation dynamics according to the features in the correlated momentum and kinetic energy distributions. In this paper, we present the quantum-mechanically calculated momentum and kinetic energy distributions of the two photoelectrons in double ionization of helium atoms driven by an XUV pulse and a weak laser pulse. The correlation patterns changes with the central photon energy of the XUV pulse. By analyzing the features of the correlation pattern, we draw different photoelectron-laser-photon interaction pictures.

2 Numerical Model

We use a one-plus-one dimensional TDSE model [13,14,15,16,17] to simulate the double ionization of helium atoms driven by a linearly polarized XUV pulse and a linearly polarized laser pulse. Limited by this model, the motion of the two electrons is restricted to the direction of laser polarization. However, the model has provided reasonable double ionization processes and successfully reproduced many double ionization mechanisms that are able to explain experimental results[13,14]. The numerical solution of the two-dimensional model can provide wave function of two related electrons in coordinate space and momentum space with time evolution. The TDSE of helium atom in linearly polarized external fields is

$$-i\frac{\partial}{\partial t}\Psi(x,y,t) = H(x,y,t)\Psi(x,y,t). \quad (1)$$

Atomic units are used throughout this paper unless otherwise stated. The total hamiltonian

$$H = H_0 + V_{int}, \quad (2)$$

where the field-free hamiltonian

$$H_0(x,y,t) = -\frac{1}{2}\frac{\partial^2}{\partial x^2} - \frac{1}{2}\frac{\partial^2}{\partial y^2} - \frac{2}{\sqrt{x^2+a^2}} - \frac{2}{\sqrt{y^2+a^2}} + \frac{1}{\sqrt{(x-y)^2+b^2}}, \quad (3)$$

including electron-nuclear attractive potentials and electron-electron repulsive potential, and the interactions between the two electrons and the external XUV and laser electric fields are

$$V_{int} = (x+y)[E_{XUV}(t) + E_L(t)]. \quad (4)$$

Here x, y are the coordinates of the two electrons, respectively. $E_L(t)$ is the electric field of a 400 nm laser pulse with a total duration of 200 optical cycles. The softcore Coulomb parameters a and b are chosen to be 1 in this work. We assume that both the XUV and laser electric fields have a sine squared temporal envelope,

$$E_\alpha(t) = E_{0,\alpha} \sin^2\left(\frac{\pi t}{T_\alpha}\right) \cos(\omega_\alpha t) \quad (5)$$

for $0 \leq t \leq T_\alpha$ and $E_\alpha = 0$ for $t > T_\alpha$, where the index α stands for XUV or L and $E_{0,\alpha}$, T_α and ω_α denote the electric-field amplitudes, pulse lengths and frequencies of the two pulses, respectively. For this helium atom model, the two-electron ground state has been obtained by imaginary-time propagation under the field-free hamiltonian and its energy $E_g = -2.24$ (-61 eV). The first ionization potential is 0.44. The two-electron wave function propagates in a large box of 480×480 with a spatial step of 0.23 and a time step of 0.1. Following Ref. [14], the two dimensional coordinate space is partitioned into two outer regions, (A) $|x| < d$, or $|y| < d$ and (B) $|x|, |y| \geq d$, with $d = 150$. The final results are insensitive to the choice of d ranging from 100 to 200. The wave function in region A propagates under the action of the total hamiltonian. In region B, which corresponds to double ionization, all the Coulomb interactions are neglected and the time evolution of the wave function can be performed simply by multiplications in momentum space. The two regions are smoothly divided by a splitting technique [14]. At the end of the propagation, the wave function in region B yields the two-electron momentum and energy distributions. After the end of the pulse, the wave function is allowed to propagate without external fields for a long time such that the final results do not change anymore. The momentum distributions of the two photoelectrons are calculated according to the following formula

$$P(p_1, p_2) = 2 |\Psi(p_1, p_2)|^2, \quad (6)$$

$\Psi(p_1, p_2)$ is two-electron wave function of the final state in momentum space. Multiplying by 2 means that the two electrons cannot be distinguished.

3 Results and Discussions

First, we present the correlated momentum and kinetic energy distributions for single-photon double ionization, as shown in Fig. 1. The circle momentum distributions is a consequence of the sharing of excess kinetic energy between the two photoelectrons. In the energy distributions, it means the sum of the kinetic energies of the two photoelectrons $E_1 + E_2 = \omega_{XUV} + E_g$. Since both the two electrons are restricted by our simulation model to move in one dimension, they can only be emitted side-by-side or back-to-back. However, our model reproduces the correlated features qualitatively with full dimensional TDSE [18, 19, 20], such as the forbidden emission for equal energy sharing in both back-to-back and side-by-side emission ($|p_1| = |p_2|$) because of the selection rule B2 discussed by Briggs and Schmidt [8] and Maulbetsch and Briggs

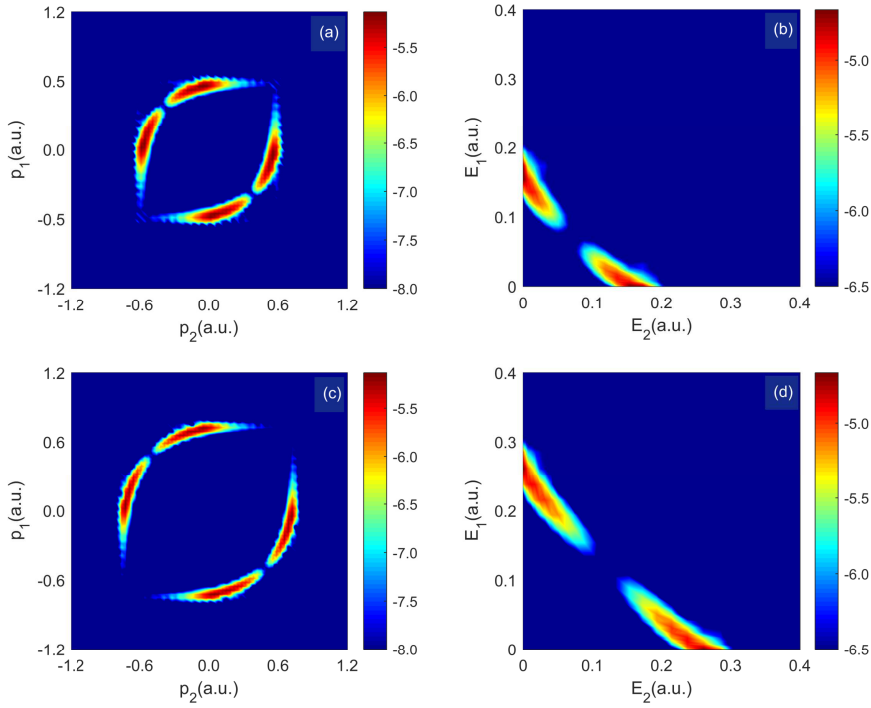


Fig. 1 Logarithmic plot of the correlated momentum (left plots) and kinetic energy (right plots) distributions of the two escaping electrons in single-photon double ionization of He. p_1 , p_2 are the final momenta of the two photoelectrons, and E_1 , E_2 the final kinetic energies, respectively. The XUV pulse has a peak intensity of 5×10^{14} W/cm² and a time duration of one hundred optical cycles. The central photon energies are 64 eV (top plots) and 67 eV (bottom plots), respectively. The units are arbitrary.

[21]. As the excess energy increases (by increasing the central XUV photon energy), the energy sharing ratio between the two photoelectrons becomes more asymmetric.

When the double ionization process is exposed to a weak laser field, the weak laser field can largely influence the double ionization probability and the correlation patterns in the momentum and kinetic energy distributions, as shown in Fig. 2 for a central XUV photon energy of 67 eV and a 400 nm laser field. As the laser field intensity increases from 1×10^{11} W/cm² (top row), to 1×10^{13} W/cm² (bottom row), the double ionization yield is enhanced by one order in magnitude for 1×10^{12} W/cm² (middle row), but then enhanced by a little for a higher intensity of 1×10^{13} W/cm² (bottom row). Furthermore, the energy sharing ratio becomes more extreme for side-by-side emission and back-to-back emission gradually dominates. The additionally emerging rings in Figs. 2(a), 2(c) and 2(e) are results of absorption or emission of one laser photon by the two photoelectrons. When the two photoelectrons absorb or emit one laser photon, the selection rule B2 is broken for equal energy sharing

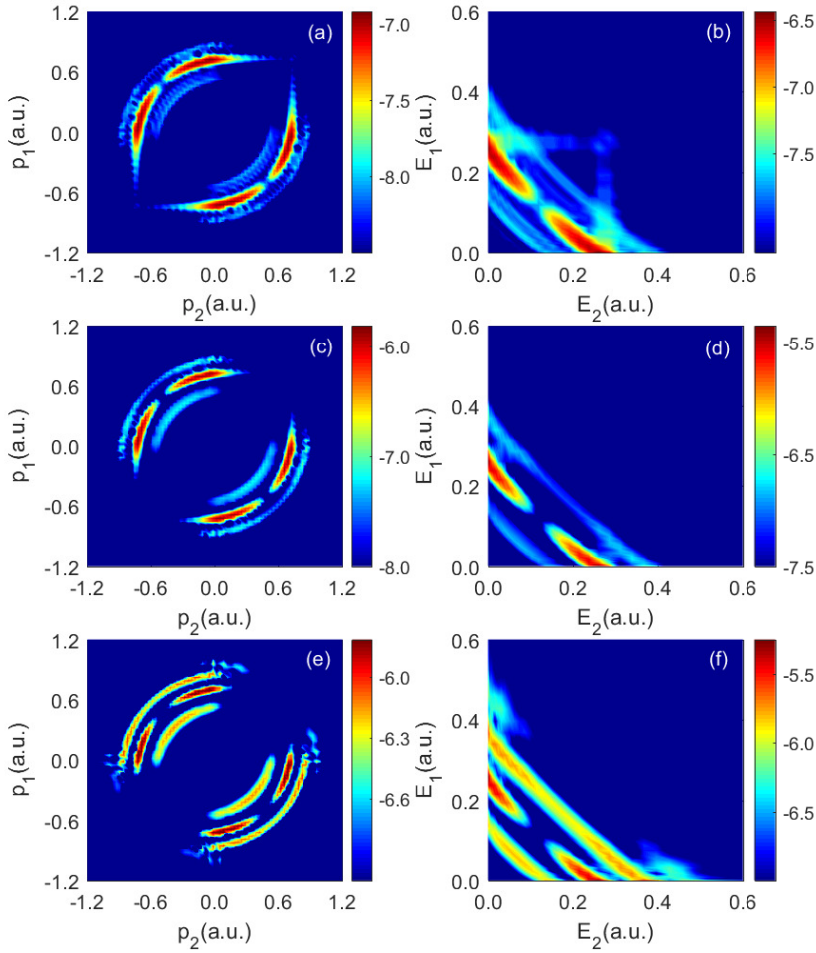


Fig. 2 Logarithmic plot of the correlated momentum (left plots) and kinetic energy (right plots) distributions of the two escaping electrons in laser-assisted single-photon double ionization of He. The XUV pulse has a peak intensity of 1×10^{14} W/cm² and a time duration of one hundred optical cycles. The XUV central photon energy is 67 eV. The 400 nm laser pulse has a peak intensity of 1×10^{11} W/cm² (top plots), 1×10^{12} W/cm² (middle plots), 1×10^{13} W/cm² (bottom plots), respectively. The units are arbitrary.

and we can see the appearance of the two photoelectrons with the same energy in back-to-back emission [19,20]. For emission of one laser photon, the total excess energy become less and the probability with any energy sharing ratio is almost the same. While the absorption of one laser photon increases the total excess energy and the two photoelectrons intend to share the excess energy more asymmetrically.

To gain more insights into the dependence of the electron-electron correlation in laser-assisted double ionization of helium atoms on the XUV photon

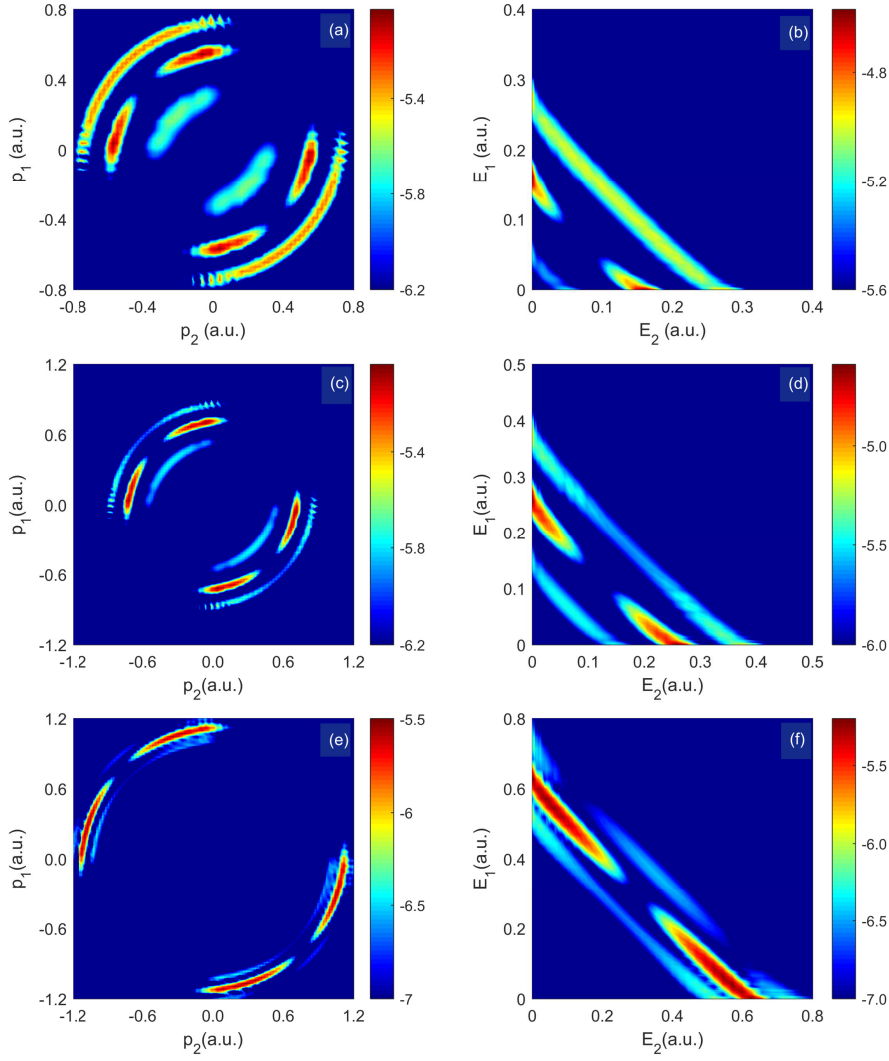


Fig. 3 Logarithmic plot of the correlated momentum (left plots) and kinetic energy (right plots) distributions of the two escaping electrons in laser-assisted single-photon double ionization of He. The XUV pulse has a peak intensity of 5×10^{14} W/cm² and a time duration of one hundred optical cycles. The XUV central photon energies are 64 eV (top plots), 67 eV (middle plots), and 77 eV (bottom plots), respectively. The 400 nm laser pulse has a peak intensity of 5×10^{12} W/cm². The units are arbitrary.

energy, i.e., the total excess energy, we change the XUV central photon energy while keeping the laser intensity unchanged. For low XUV photon energy at 64 eV, the absorption probability of one laser photon by the two photoelectrons is much larger than the emission probability of one laser photon, see Figs. 3(a) and 3(b). This is well understood since the emission of one laser photon (3 eV)

decreases the excess energy near to 0, making the electron that first absorbs one XUV photon much difficult to kick out the other through energy transferring. As the XUV photon energy increases to 67 eV, the emission probability of one laser photon becomes approaching to the absorption probability, see Figs. 3(c) and 3(d). The asymmetric energy sharing ratio is preferable for the laser-photon absorption channel. As the XUV photon energy further increases to 77 eV, the asymmetric energy sharing ratio is preferable for the laser-photon emission channel. In contrast, the equal energy sharing ratio is preferred for the laser-photon absorption channel, see Fig. 3(f). More surprisingly, forbidden emission of the two photoelectrons appears in some asymmetric energy sharing regions for the laser-photon absorption channel, which is never found in previous work.

The above dependence of the correlated energy distributions on XUV photon energy and the weak laser field can be explained based on the kick-out double ionization mechanism. In kick-out double ionization mechanism, one electron absorbs one XUV photon (we refer to this electron as the first electron) and then transfers energy to the other one (the second electron) through Coulomb repulsion, kicking the other one out from the nucleus. When the two electrons are exposed to a weak laser field, another energy transferring channel is open. In this channel, the first electron emits one laser photon into the laser field, while the second one absorbs one laser photon from the laser field. Here the laser field acts as an energy transferring field. No net laser photon participates into the double ionization process, but the additional energy transferring channel enhances double ionization probability dramatically.

When the first electron additionally absorbs one laser photon and the other does not absorb or emits one laser photon, see Fig. 4(a), the final kinetic energy of the first electron will be larger than that of the second one. Conversely, see Fig. 4(b), the difference in final kinetic energies between the two electrons becomes small and they can have the same kinetic energy. For the case of the laser photon emission, see Figs. 4(c) and 4(d), the similar explain also works. There are two channels for the laser-photon absorption. One channel is that the first electron absorbs one laser photon, the energy of the second electron $E_2 \in [0, E_{2,max}]$, where $E_{2,max}$ is the maximum kinetic energy, less than half the total excess kinetic energy. The other channel is that the second electron absorbs one laser photon, the energy of the second electron $E_2 \in [\omega_L, E_{2,max} + \omega_L]$. There is an overlap energy region for the two channels if $E_{2,max} > \omega_L$. The two double ionization channels interfere in the overlap energy region. If $E_{2,max}$ is much larger than ω_L , fully destructive interference happens.

4 Conclusion

We investigated two-color two-photon double ionization of a helium model atom driven by a XUV pulse and a weak laser pulse. By numerically solving a one-plus-one dimensional TDSE model, we calculated the correlated mo-

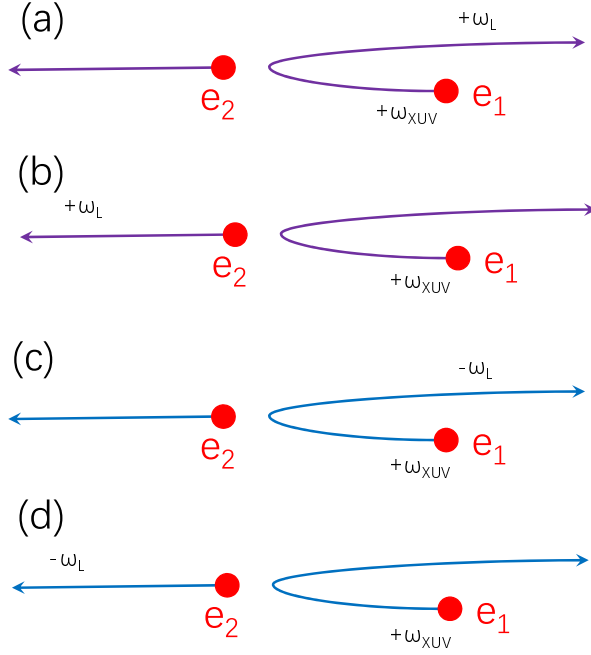


Fig. 4 Schematic diagram of the absorption and emission of one laser photon by one of the two escaping electrons in single-photon double ionization of He. ω_L and ω_{XUV} are the central photon energies of the weak laser field and the XUV laser field, respectively. e_1 represents the first electron that absorbs one XUV photon and e_2 the second electron that kicked out from the nucleus by the first electron.

momentum and kinetic energy distribution of the two photoelectrons. The weak assisting laser field provides an energy transferring channel, increasing double ionization probability remarkably for single-XUV-photon double ionization. The participation of the laser photon into the double ionization dramatically changes the correlation patterns in the momentum and kinetic energy distributions. Such changes depend on the XUV photon energy, the laser intensity and how the laser photon interacts with the two electrons. Our work provides instructions in revealing dynamics details of single-photon double ionization and manipulating the electronic correlation in double ionization.

Funding. National Natural Science Foundation, China (11674257, 11604248, 11874019); Program for Distinguished Middle-aged and Young Innovative Research Team in Higher Education of Hubei, China (T201806); Natural Science Foundation of Hubei Province, China (2020CFA082).

References

1. O. Schwarzkopf, B. Krässig, J. Elmiger, and V. Schmidt, "Energy- and angle-resolved double photoionization in helium," *Phys. Rev. Lett.* **70**, 3008-3011 (1993).
2. O. Schwarzkopf and V. Schmidt, "Experimental determination of the absolute value of the triple differential cross section for double photoionization in helium," *J. Phys. B: At. Mol. Opt. Phys.* **28**, 2847-2862 (1996).
3. H. Bräuning, R. Dörner, C. L. Cocke, M. H. Prior, B. Krässig, A. S. Kheifets, I. Bray, A. Bräuning-Demian, K. Carnes, S. Dreuil, V. Mergel, P. Richard, J. Ullrich, and H. Schmidt-Böcking, "Absolute triple differential cross sections for photo-double ionization of helium-experiment and theory," *J. Phys. B: At. Mol. Opt. Phys.* **31**, 5149-5160 (1998).
4. D. N. Fittinghoff, P. R. Bolton, B. Chang, and K. C. Kulander, "Observation of nonsequential double ionization of helium with optical tunneling," *Phys. Rev. Lett.* **69**, 2642 (1992).
5. B. Walker, B. Sheehy, L. F. DiMauro, P. Agostini, K. J. Schafer, and K. C. Kulander, "Precision Measurement of Strong Field Double Ionization of Helium," *Phys. Rev. Lett.* **73**, 1227-1230 (1994).
6. Th. Weber, H. Giessen, M. Weckenbrock, G. Urbasch, A. Staudte, L. Spielberger, O. Jagutzki, V. Mergel, M. Vollmer, and R. Dörner, "Correlated electron emission in multiphoton double ionization," *Nature (London)* **405**, 658-661 (2000).
7. F. Maulbetsch and J. S. Briggs, "Angular distribution of electrons following double photoionization," *J. Phys. B: At. Mol. Opt. Phys.* **26**, 1679-1696 (1993).
8. J. S. Briggs and V. Schmidt, "Differential cross sections for photo-double-ionization of the helium atom," *J. Phys. B: At. Mol. Opt. Phys.* **33**, R1-R48 (2000).
9. J. S. Parker, L. R. Moore, K. J. Meharg, D. Dundas, and K. T. Taylor, "Double-electron above threshold ionization of helium," *J. Phys. B: At. Mol. Opt. Phys.* **34**, L69 (2001).
10. L. Avaldi and A. Huetz, "Photodouble ionization and the dynamics of electron pairs in the continuum," *J. Phys. B: At. Mol. Opt. Phys.* **38**, S861-S891 (2005).
11. W. C. Jiang, L. Y. Peng, W. H. Xiong, and Q. Gong, "Comparison study of electron correlation in one-photon and two-photon double ionization of helium," *Phys. Rev. A* **88**, 023410 (2013).
12. A. Rudenko, L. Foucar, M. Kurka, Th. Ergler, K. U. Kühnel, Y. H. Jiang, A. Voitkiv, B. Najjari, A. Kheifets, S. Lj̇udemann, T. Havermeier, M. Smolarski, S. Schössler, K. Cole, M. Schöffler, R. Ḋorner, W. Li, B. Keitel, R. Treusch, M. Gensch, C. D. Schröter, R. Moshhammer, and J. Ullrich, "Recoil-Ion Momentum Distributions for Two-Photon Double Ionization of He and Ne by 44 eV Free-Electron Laser Radiation," *Phys. Rev. Lett.* **101**, 073003 (2008).
13. M. Lein, E. K. U. Gross, and V. Engel, "Intense-Field Double Ionization of Helium: Identifying the Mechanism," *Phys. Rev. Lett.* **85**, 4707 (2000).
14. Q. Liao and P. Lu, "Energy correlation in above-threshold nonsequential double ionization at 800 nm," *Phys. Rev. A* **82**, 021403 (2010).
15. Q. Liao, Y. Zhou, C. Huang, and P. Lu, "Multiphoton Rabi oscillations of correlated electrons in strong-field nonsequential double ionization," *New J. Phys.* **14**, 013001 (2012).
16. Q. Liao, Ye Li, M. Qin, and P. Lu, "Attosecond interference in strong-field nonsequential double ionization," *Phys. Rev. A* **96**, 063408 (2017).
17. K. Liu, M. Qin, Q. Li, Q. Liao, "Transition from strong-field sequential to nonsequential double ionization at near-infrared wavelengths and low intensities," *Opt. Quantum Electron.* **50**, 364 (2018).
18. X. Guan, K. Bartschat, and B. I. Schneider, "Dynamics of two-photon double ionization of helium in short intense XUV laser pulses," *Phys. Rev. A* **77**, 043421 (2008).
19. A. Liu and Uwe Thumm, "Laser-assisted XUV few-photon double ionization of helium: Joint angular distributions," *Phys. Rev. A* **89**, 2684-2690 (2014).
20. A. Liu and Uwe Thumm, "Laser-assisted XUV double ionization of helium: Energy-sharing dependence of joint angular distributions," *Phys. Rev. A* **91**, 043416 (2015).
21. F. Maulbetsch and J. S. Briggs, "Selection rules for transitions to two-electron continuum state," *J. Phys. B: At. Mol. Opt. Phys.* **28**, 551 (1995).

Figures

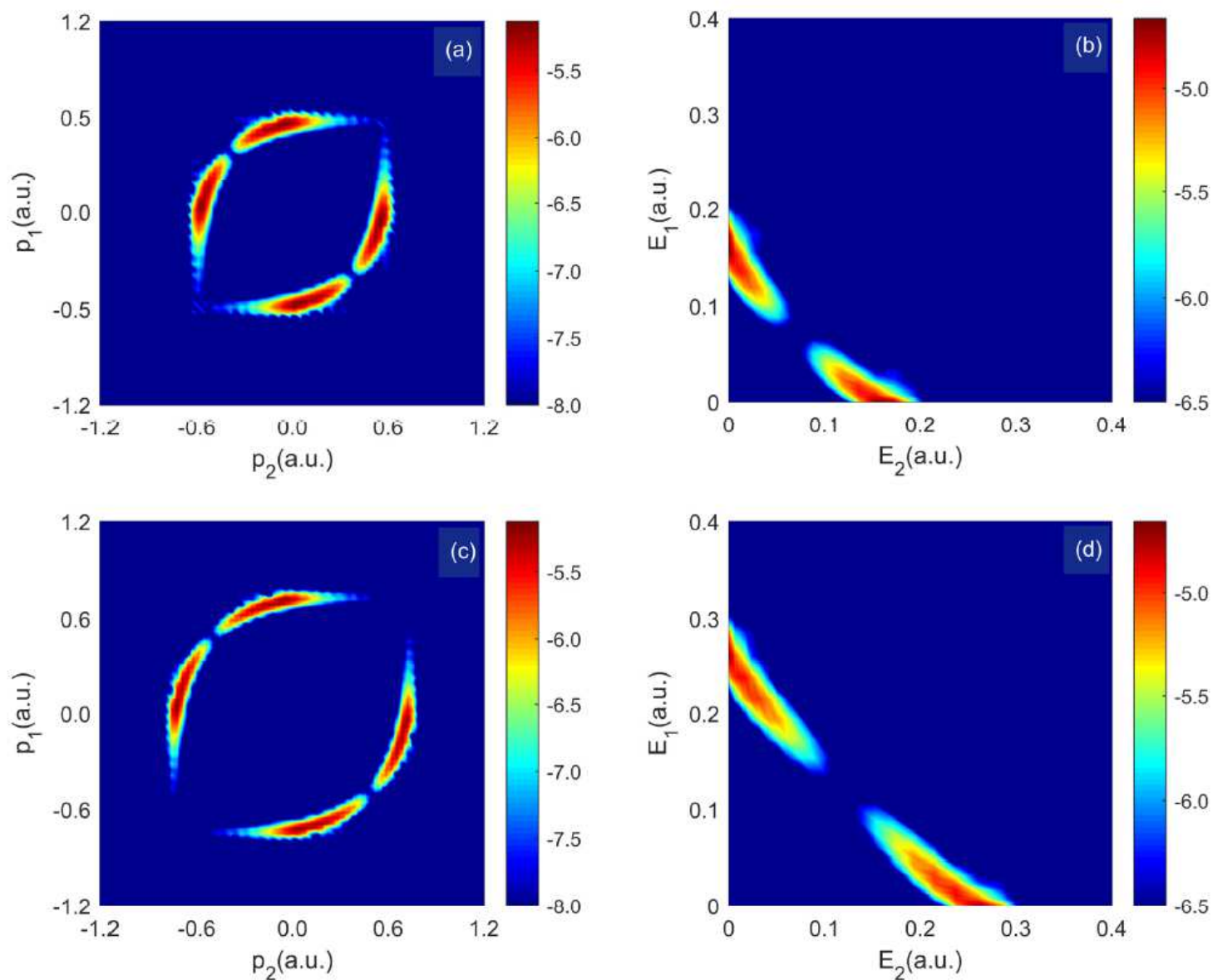


Figure 1

Logarithmic plot of the correlated momentum (left plots) and kinetic energy (right plots) distributions of the two escaping electrons in single-photon double ionization of He. p_1 , p_2 are the final momenta of the two photoelectrons, and E_1 , E_2 the final kinetic energies, respectively. The XUV pulse has a peak intensity of 5×10^{14} W/cm² and a time duration of one hundred optical cycles. The central photon energies are 64 eV (top plots) and 67 eV (bottom plots), respectively. The units are arbitrary.

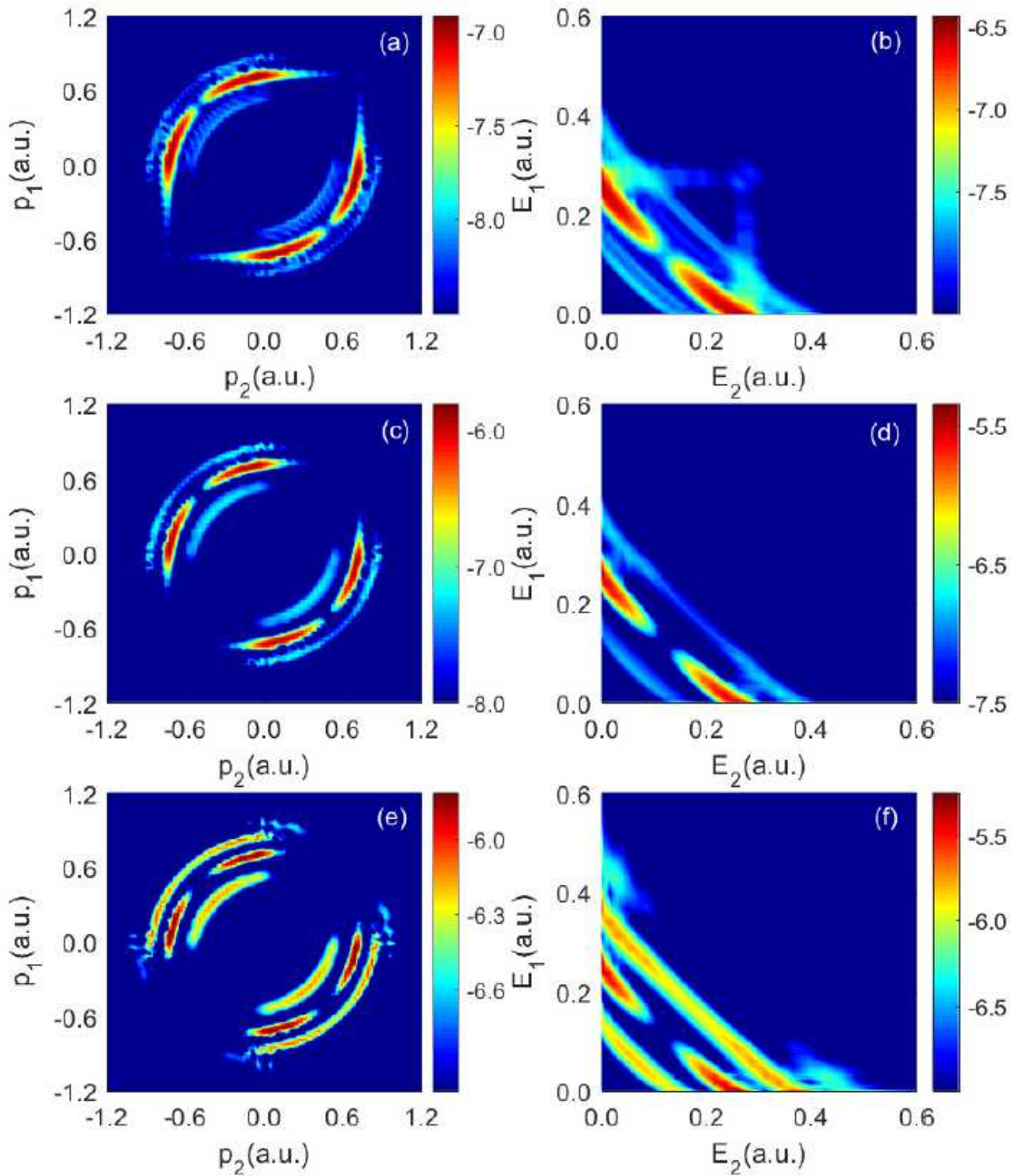


Figure 2

Logarithmic plot of the correlated momentum (left plots) and kinetic energy (right plots) distributions of the two escaping electrons in laser-assisted single-photon double ionization of He. The XUV pulse has a peak intensity of 1×10^{14} W/cm² and a time duration of one hundred optical cycles. The XUV central photon energy is 67 eV. The 400 nm laser pulse has a peak intensity of 1×10^{11} W/cm² (top plots), 1×10^{12} W/cm² (middle plots), 1×10^{13} W/cm² (bottom plots), respectively. The units are arbitrary.

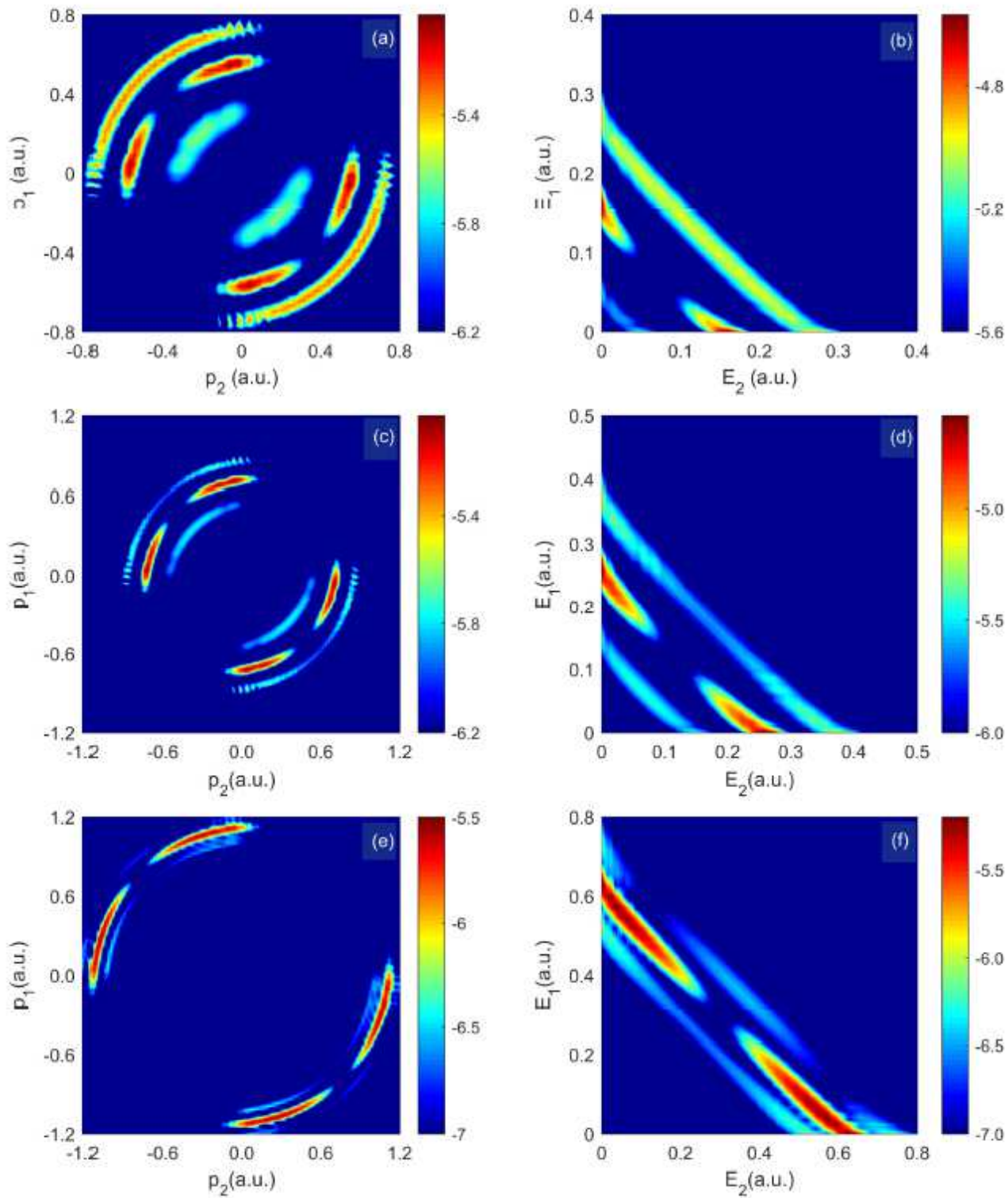


Figure 3

Logarithmic plot of the correlated momentum (left plots) and kinetic energy (right plots) distributions of the two escaping electrons in laser-assisted single-photon double ionization of He. The XUV pulse has a peak intensity of 5×10^{14} W/cm² and a time duration of one hundred optical cycles. The XUV central photon energies are 64 eV (top plots), 67 eV (middle plots), and 77 eV (bottom plots), respectively. The 400 nm laser pulse has a peak intensity of 5×10^{12} W/cm². The units are arbitrary.

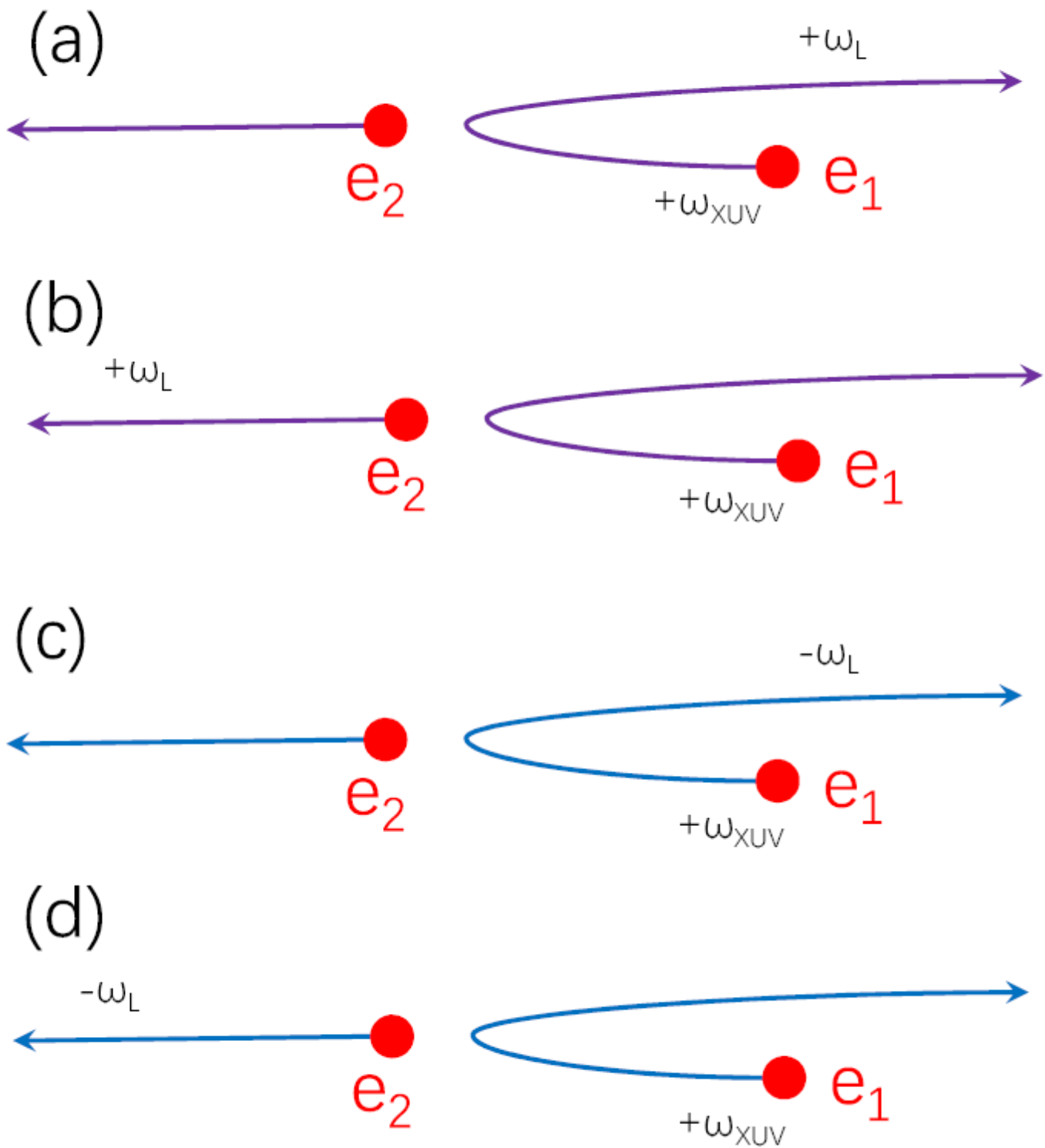


Figure 4

Schematic diagram of the absorption and emission of one laser photon by one of the two escaping electrons in single-photon double ionization of He. ω_{L} and ω_{XUV} are the central photon energies of the weak laser field and the XUV laser field, respectively. e_1 represents the first electron that absorbs one XUV photon and e_2 the second electron that kicked out from the nucleus by the first electron.